JOURNAL OF Materials CHEMISTRY

Restructuring of mesoporous silica: high quality large crystal MCM-41 *via* a seeded recrystallisation route†

Robert Mokaya,* Wuzong Zhou and William Jones

Department of Chemistry, University of Cambridge, Lensfield Road, Cambridge, UK CB2 1EW. Tel: +44 (0)1223-33 64 65; Fax: +44 (0)1223-33 63 62; E-mail: rm140@cus.cam.ac.uk

Received 10th January 2000, Accepted 14th February 2000
Published on the Web 17th March 2000

Post-synthesis recrystallisation of calcined small crystallite MCM-41 has been used to prepare highly ordered large crystallite MCM-41 materials in a two step synthesis route. The calcined small crystallite 'primary' MCM-41, obtained from the first step, is used as the 'silica source' in an otherwise normal secondary synthesis or recrystallisation procedure. During the secondary synthesis the calcined primary MCM-41 crystallites are preserved and act as seeds for further crystal growth; the real source of the silicate ions required for crystal enlargement is amorphous silica which is part of the primary MCM-41 yield. In addition to having larger crystallites, the resulting 'secondary' MCM-41 exhibits much better long range structural ordering as observed by powder XRD and TEM. The recrystallisation causes a modest increase in basal (d_{100}) spacing and a decrease in pore size resulting in thicker pore walls and a slight decrease in surface area and pore volume. These structural changes are accompanied by a morphological transformation from spherical particles to larger sheet or plate like domains. TGA, ^{29}Si NMR, SEM and powder XRD studies provide strong evidence for a seeding mechanism.

Introduction

Porous inorganic solids with uniform and well ordered mesopores are much in demand for use in catalytic processes or separations involving large molecules which are beyond the range of microporous zeolites. The synthesis of truly mesoporous silicas *via* a mechanism in which supramolecular assemblies of surfactant micelles (so-called liquid crystal templates) act as structure directors for the organisation of inorganic silicate precursors has therefore opened up a new and exciting field in materials science research.[1] Considerable research effort has recently been focused on improving the long range structural ordering and on tailoring the textural properties of these mesoporous silicas. For example the diameter of the hexagonally packed one dimensional pore channels of the mesoporous molecular sieve MCM-41 can be tailored in the 15–100 Å range. In purely siliceous MCM-41 the pore size may be controlled by a variety of methods which include using templating surfactant molecules with varying alkyl chain lengths,[2–4] or adding auxiliary organic molecules which are solubilised in the hydrophobic region of the templating aggregates thus increasing micellar size.[2,5,6] In most cases, however, the use of expander molecules or very long alkyl chain surfactants is usually accompanied by an undesirable diminution in long range structural ordering.[2–6] More recently it has been shown that the pore size (and in some cases long range order) of MCM-41 can be increased *via* hydrothermal restructuring of the as-synthesised (surfactant containing) material in the mother liquor[7–10] or water.[11,12] Such hydrothermal treatments have been reported to result in an improvement or decrease in structural ordering depending on the prevailing synthesis and/or post-synthesis restructuring conditions.[7–12] The pore size uniformity or long range structural ordering of MCM-41 can also be improved by controlling the pH of the synthesis gel (by repeated addition of acid to the synthesis gel during hydrothermal crystallisation) such that the silicate polymerisation equilibrium is shifted towards the formation of MCM-41 mesophase.[13,14]

We have recently reported on a two-step synthesis approach for the preparation of well ordered large MCM-41 crystallites which, in the second step, involves the use of calcined MCM-41 as the 'silica source' for secondary synthesis or recrystallisation.[15] With the exception of our aforementioned report,[15] all other previous attempts at improving the long range structural ordering of MCM-41 have involved secondary (or post-synthesis) treatments or modifications to the as-synthesised (surfactant containing) material[7–12] and to the best of our knowledge there has been no other report on secondary synthesis utilising calcined or template free MCM-41. Furthermore there have been very few reports on attempts to control or increase the crystal size of MCM-41 despite the fact that control of crystal size may well be crucial to the use of MCM-41 materials in thin film applications (such as in separation membranes), as host for the fabrication of molecular wires or as solid acid catalysts. The apparent lack of research efforts aimed at increasing the crystal size of MCM-41 may be due to the assumption that, compared to multi-dimensional pore molecular sieves (*e.g.*, MCM-48 for which large crystallites have been reported),[16] the formation of large MCM-41 crystals would be difficult due to its one-dimensional channel structure which is subject to bending and fracture. Our preliminary characterisation of the recrystallised MCM-41 materials prepared *via* the two-step synthesis process[15] showed improved long range structural ordering and a marked increase in crystal size. Here we give a full account of the properties of the recrystallised MCM-41 and expand on our hitherto proposed seeded (secondary synthesis) or recrystallisation mechanism.

Experimental

Synthesis of materials

In step 1, the parent MCM-41 material (herein referred to as the primary MCM-41) was prepared as follows: tetramethyl-

†Electronic supplementary information (ESI) available: SEM images of samples MCM-41(96) as prepared and after recrystallisation for 48 and 96 hours. See http://www.rsc.org/suppdata/jm/b0/b000179l/

DOI: 10.1039/b000179l

ammonium hydroxide (TMAOH) and cetyltrimethyammonium bromide (CTAB) were dissolved in distilled water by stirring at 35 °C. The silica source, fumed silica (Sigma), was added to the solution under stirring for 1 hour. After further stirring for 1 hour the resulting synthesis gel of composition SiO_2 : 0.25 CTAB : 0.2 TMAOH : 40 H_2O was left to age for 20 hours at room temperature following which the mixture was transferred to a Teflon-lined autoclave and heated at 150 °C for 48 hours. The solid product was obtained by filtration, washed with distilled water, dried in air at room temperature and calcined at 550 °C for 8 hours to yield the primary MCM-41. For step 2 (secondary synthesis) a synthesis gel of molar ratio as above was assembled except that the primary MCM-41 was used as the 'silica source' instead of the fumed silica. The experimental procedures were exactly as described above for the primary synthesis. The MCM-41 yield, based on silica recovery, was *ca.* 60% for the primary synthesis and >90% for the secondary synthesis.

Characterisation

Powder X-ray diffraction (XRD) patterns were recorded using a Philips 1710 powder diffractometer with Cu-Kα radiation (40 kV, 40 mA), 0.02° step size and 1 s step time. Thermogravimetric analysis (TGA) was performed using a Polymer Laboratories TG 1500 analyser with a heating rate of 20 °C min^{-1} under a nitrogen flow of 25 ml min^{-1}. ^{29}Si (MAS) NMR spectra were acquired at 79.4 MHz using a Chemagnetics CMX-400 spectrometer and 7.5 mm diameter zircona rotors spun at 3.2 kHz. 60° pulses and 500 s recycle delays were used. Chemical shifts are given as δ from external tetramethylsilane (TMS). Textural properties (surface area and pore volume) were determined at −196 °C using nitrogen in a conventional volumetric technique by a Coulter SA3100 sorptometer or a Micromeritics ASAP 2400 sorptometer. Before analysis the previously calcined samples were oven dried prior to evacuation overnight at 200 °C under vacuum. The surface area was calculated using the BET method based on adsorption data in the partial pressure (P/P_o) range 0.05 to 0.2 and the pore volume was determined from the amount of N_2 adsorbed at P/P_o = *ca.* 0.99. The calculation of pore size was performed using the Barrett–Joyner–Halenda (BJH) method applied to the adsorption data of the N_2 sorption isotherms.

Transmission electron microscopic (TEM) images were recorded using a JEOL JEM-200CX electron microscope operating at 200 kV with a modified specimen stage with objective lens parameters C_s (spherical aberration coefficient) = 0.41 mm and C_c (chromatic aberration coefficient) = 0.95 mm, giving an interpretable point resolution of *ca.* 0.185 nm. Samples for analysis were prepared by crushing the particles between two glass slides and spreading them on a holey carbon film supported on a Cu grid. The samples were briefly heated under a tungsten filament light bulb in air before transfer into the specimen chamber. The images were recorded at magnifications of 24 000× to 49 000×. Scanning electron microscopy (SEM) was performed using a JEOL JSM-820 scanning electron microscope operating at an accelerating voltage of between 5 and 15 kV. Samples were mounted using a conductive carbon double sided sticky tape. A thin (*ca.* 10 nm) coating of gold sputter was deposited onto the samples to reduce the effects of charging.

Results and discussion

The powder X-ray diffraction (XRD) patterns obtained for the calcined primary and secondary MCM-41 are shown in Fig. 1. The pattern of the primary MCM-41 is typical of a relatively well ordered material and shows an intense (100) diffraction peak and three higher order (110), (200) and (210) peaks. The secondary MCM-41 exhibits an XRD pattern which compared

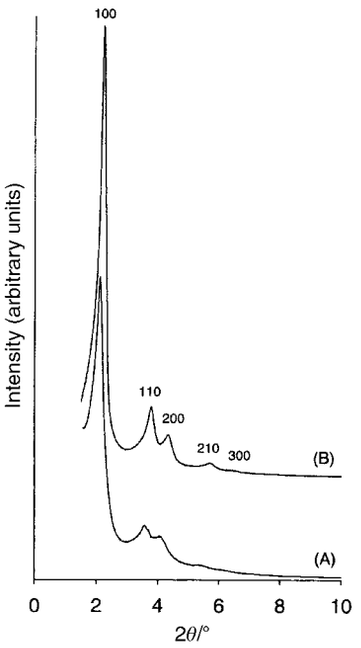

Fig. 1 Powder XRD patterns of calcined (A) primary MCM-41 and (B) secondary MCM-41.

to that of primary MCM-41 shows an increase in the intensity of the (100) peak along with an increase in intensity and improvement in the resolution of the higher order peaks. In addition some extra higher order peaks (*i.e.*, (300) and a diffuse (220/310) peak) are observed. We note that these higher order peaks are seldom observed even in benchmark good quality MCM-41.[14,17] The XRD pattern for secondary MCM-41 therefore suggests an improvement in long range ordering (more and better resolved higher order peaks) and an enlargement in scattering domain (or crystal) size as indicated by the increase in peak intensities and associated reduction in full widths at half maxima (FWHM). There is only a slight shift in the 2θ value of the (100) peak indicating that secondary synthesis does not have a significant effect on the final basal (d_{100}) spacing of the calcined samples.

A typical TEM image obtained for secondary MCM-41 together with a corresponding selected area electron diffraction (SAED) pattern (bottom inset) are shown in Fig. 2. The main TEM image which 'captures' a whole 'particle' clearly illustrates the enlargement of crystal size. A direct measurement of crystallite size from TEM images indicated that the crystal size of primary MCM-41 is in the range 40 to 60 nm with a peak at 45 nm which is similar to other standard MCM-

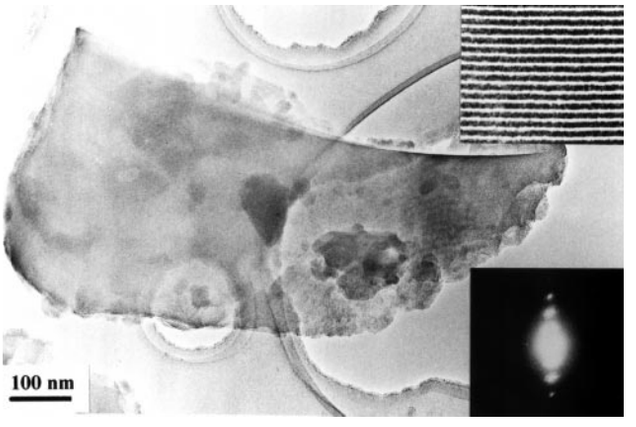

Fig. 2 Representative TEM image and corresponding SAED pattern (bottom inset) of a large crystal of secondary MCM-41. The top inset is an enlarged version of the image showing highly ordered channels.

41 specimens presented in previous reports. Indeed no crystallites larger than 100 nm were observed for primary MCM-41. On the other hand the crystal size of secondary MCM-41 was in the range 400 to 800 nm and crystallites smaller than 100 nm were not observed. The significant improvement in the crystallinity for the secondary MCM-41 is clearly indicated by the SAED pattern where four or more pairs of diffraction spots appear along the (100) or (110) direction as opposed to one or two pairs observed for primary MCM-41 crystallites. This is in accord with the excellent ordering of the pore channels shown in Fig. 2 (top inset).

The increase in crystal or particle size observed for the secondary MCM-41 is accompanied by an apparent transformation in morphology. Fig. 3 and 4 show SEM images obtained for primary and secondary MCM-41 at various magnifications. The primary MCM-41 is made up of sub-micrometre sized free standing or aggregated sphere shaped particles (Fig. 3a and 4a) which is the typical morphology of normal MCM-41 synthesised under basic conditions. Indeed we observed virtually no other particle morphology for primary MCM-41. On the other hand the morphology of secondary MCM-41 differs from that of the primary MCM-41 in that it is made up of larger sheet or plate-like particles. The sheet-like and flaky nature of secondary MCM-41 particles is clearly observed in Fig. 3b. In some cases, as shown in Fig. 3c and d, the sheet-like particles appear to extend over large areas giving a membrane or film-like appearance. As far as we know this is the first time that such particle morphology has been reported for MCM-41 prepared under basic conditions. Fig. 4 shows SEM images for primary and secondary MCM-41 obtained at lower magnification and clearly illustrates the contrast in particle morphology between the two samples. It is interesting to note that the sheet-like particles of secondary MCM-41 extend for up to 15 μm. We note that a sheet-like particle morphology for secondary MCM-41 is consistent with the shape of its crystallites observed under TEM (see Fig. 1). Indeed attempts to image the pore channels of secondary MCM-41 along the pore axis were largely unsuccessful presumably due to the tendency of the sheet-like particles to lie flat rather than edge on.

The N_2 sorption isotherms for the primary and secondary MCM-41 materials are shown in Fig. 5 and Table 1 gives the corresponding textural properties. Both samples exhibit similar isotherms with a well developed step in the relative pressure (P/P_o) range 0.35 to 0.45 characteristic of capillary condensation (filling) into uniform mesopores. The isotherms are in good agreement with the XRD patterns in Fig. 1 and confirm that both samples possess good structural ordering and a narrow pore size distribution. It is, however, worth noting that a comparison of the XRD patterns and N_2 sorption isotherms indicates that XRD is more sensitive to the structural changes occasioned by the recrystallisation; the improvement in long-range ordering is more clearly illustrated by the XRD patterns than in the N_2 sorption isotherms. Secondary synthesis results in a slight shift to lower pore size (pore filling step at lower P/P_o) which is confirmed in Table 1 by the average pore size obtained from BJH analysis of sorption data. The decrease in pore size is accompanied by a modest increase in basal (d_{100}) spacing and lattice parameter (a_o) which results in thicker pore walls for secondary MCM-41. We note that the calculation of pore size by applying the BJH model to the desorption data (see Table 1) underestimates the pore size with the conseqence that the implied wall thickness may be too high; this does not, however, affect the trend observed. The thicker walls of secondary MCM-41 are, as expected, accompanied by slightly lower surface area and pore volume.

It is clear from the results discussed above that the restructuring which occurs during secondary synthesis results in an improvement in long range order and an increase in the crystal (or particle) size which are accompanied by morphological transformation. Information concerning the processes responsible for these changes has been obtained. Fig. 6 shows the thermogravimetric analysis (TGA) curves for the as-synthesised samples. The curves indicate that the amount of template occluded by the secondary MCM-41 is less (by *ca.* 18%) than for the primary MCM-41 and therefore that the surfactant/silica ratio is lower for as-synthesised secondary MCM-41. Indeed the calculated ratio between the occluded template (weight loss between 120 and 350 °C) and residual

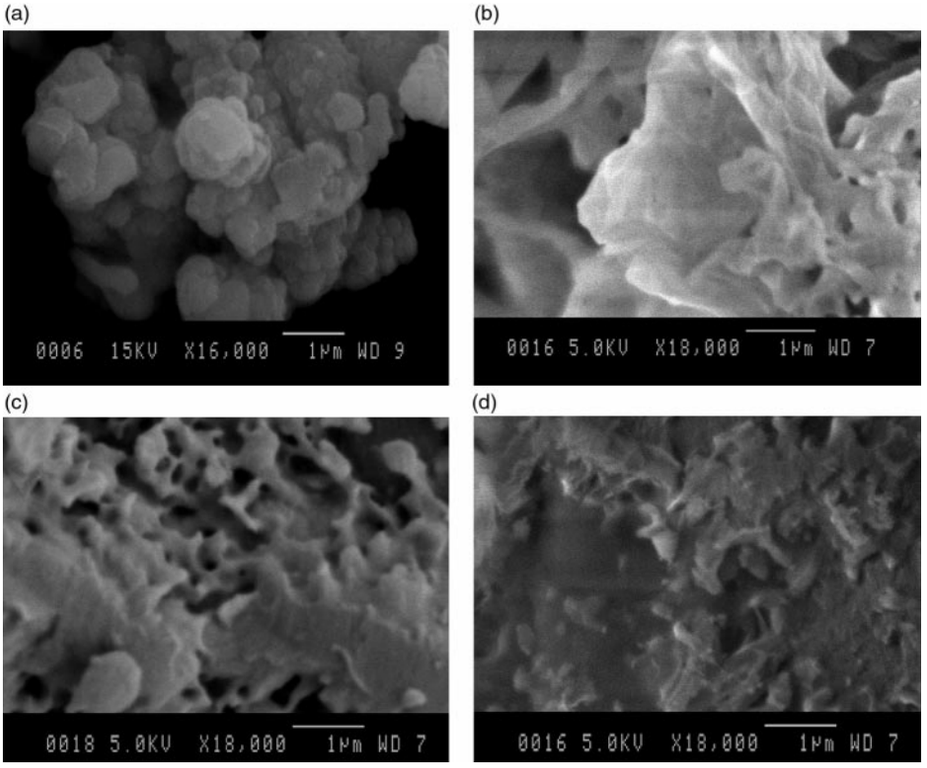

Fig. 3 Representative SEM micrographs of (a) primary (1°) MCM-41 and (b, c and d) secondary (2°) MCM-41.

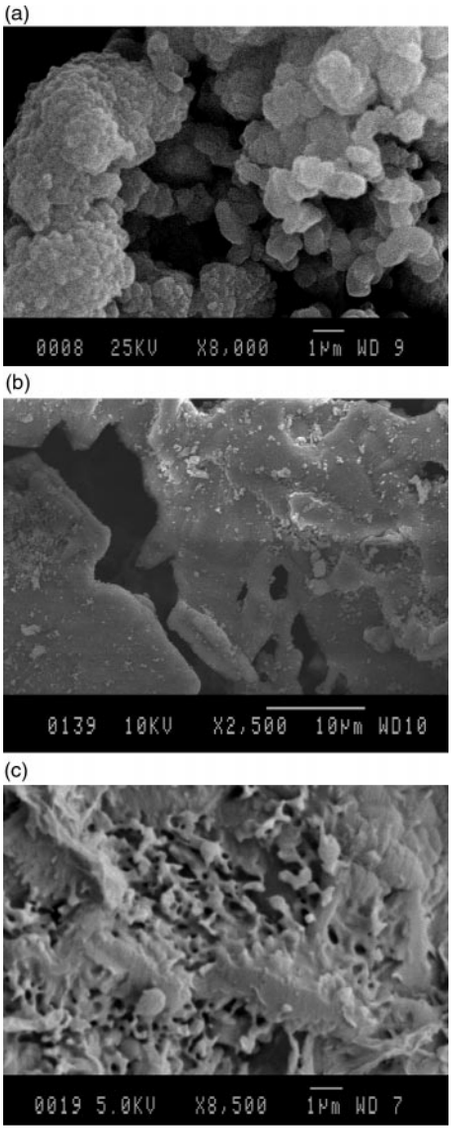

Fig. 4 Representative SEM micrographs of (a) primary (1°) MCM-41 and (b and c) secondary (2°) MCM-41.

silica weight (at 1000 °C) expressed as the CTMA/SiO_2 molar ratio was 0.17 and 0.13 for primary and secondary MCM-41 respectively. A lower amount of surfactant is retained in the secondary MCM-41 silica/surfactant mesophase which implies that less template is required or 'used up' during the secondary synthesis step. This would be the case if the primary MCM-41 (which is the silica source) remains largely intact during the secondary synthesis step with its crystallites acting as 'seeds' or starting points for further crystal growth. In this scenario the real source of silicate ions for the observed crystallite enlargement is amorphous silica which is usually part of any MCM-41 yield.

Further crystal growth during secondary synthesis must be preceded by the dissolution of the silica source. The dissolution is made possible by the presence of OH^- ions from TMAOH.[17] The OH ions are used up during the dissolution and therefore the extent to which the concentration of OH ions (or pH) reduces during the crystallisation period is a measure of the amount or extent of dissolution.[17] For the primary synthesis we observed a decrease in pH from 12.4 to 11.5 after ageing for 20 hours at room temperature and a further decrease to 10.7 after crystallisation at 150 °C for 48 hours. In contrast the gel for secondary synthesis (with primary MCM-41 as the 'silica source') had a pH of 11.5 which remained largely unaffected by ageing at room temperature and reduced only slightly to 11.2

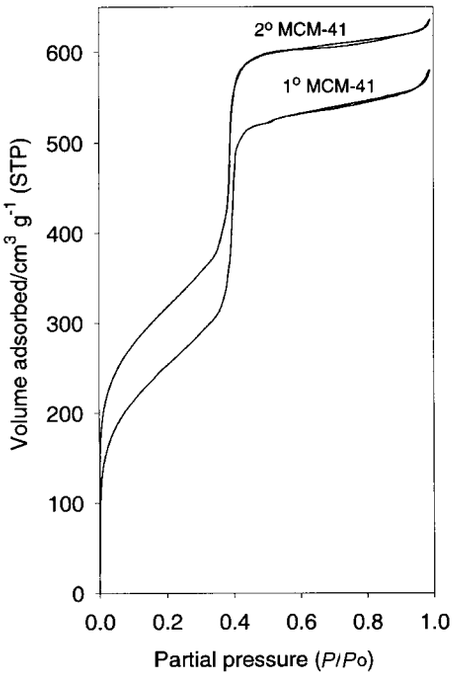

Fig. 5 Nitrogen sorption isotherms of primary (1°) MCM-41 and secondary (2°) MCM-41. For clarity the isotherm of 2° MCM-41 is offset (*y*-axis) by 50.

after crystallisation for 48 hours at 150 °C. We attribute the smaller overall reduction in pH during secondary synthesis to the dissolution of comparatively less silica. In other words if the primary MCM-41 crystallites had dissolved as extensively (and to the same extent) as the dissolution of the amorphous fumed silica (during the primary synthesis), the decrease in pH would have been as great as that observed during the primary synthesis. We tested the validity of using the decrease in pH as a measure of silica dissolution by performing secondary synthesis in which the silica source was made up of 50% primary MCM-41 and 50% amorphous fumed silica. All other synthesis parameters were as detailed in the Experimental section. The initial pH of 12.0 decreased to 11.6 after ageing at room temparature for 20 hours and finally reduced to 11.0 after crystallisation at 150 °C for 48 hours. The pH changes are clearly intermediate between those of primary synthesis and secondary synthesis which is what is expected for an intermediate amount of amorphous silica in the synthesis gel. Assuming that all the amorphous silica is dissolved, this is consistent with our assumption that the pH changes are linked to the extent of silica dissolution. This observations along with the higher silica recovery (>90% for secondary synthesis compared to *ca.* 60% for primary synthesis) are a strong indication that the primary MCM-41 was preserved during the secondary synthesis. The small decrease in pH during secondary synthesis is attributable to the dissolution of amorphous silica phase present in the primary MCM-41 and which provides the silicate units for further crystal growth as discussed later. We note that a gel comprising the primary MCM-41 and CTAB (*i.e.*, without TMAOH) had a pH of 2.0 which increased to 4.8 after the hydrothermal treatment and resulted in the complete destruction of the MCM-41. It appears therefore that the primary MCM-41 crystallites are stable at a pH of $\approx$11 in the presence of both the surfactant and TMAOH. It is likely that the surfactant plays a key role in the stabilisation and preservation of the seed crystallites.

The TGA curves of the as-synthesised samples shown in Fig. 6 indicate that the weight loss attributable to dehydroxylation of silanol groups (between 350 and 800 °C)[4,7] is lower (by *ca.* 35%) for the secondary MCM-41. This is a clear indication that the as-synthesised secondary MCM-41 is at a

Table 1 Textural properties of the study materials

Sample	d_{100}/Å	Surface area/$m^2\ g^{-1}$	Pore volume/$cm^3\ g^{-1}$	Pore size/Å	a_o[a]/Å	Wall thickness[b]/Å
Primary MCM-41	42.8	918	0.89	38.7 (33.4)[c]	49.4	10.7 (16.0)[c]
Secondary MCM-41	44.6	880	0.81	36.4 (31.4)	51.5	15.1 (20.1)

[a]a_o = The lattice parameter, from the XRD data using the formula $a_o = 2d_{100}/\sqrt{3}$. [b]Wall thickness = a_o − pore size. [c]Values in parentheses are pore size and corresponding wall thickness obtained from BJH analysis of desorption data.

much higher level of silicate polymerisation compared to its primary analogue. The higher level of silica condensation in secondary MCM-41 is clearly illustrated in Fig. 7 which shows the ^{29}Si MAS NMR spectra of the as-synthesised (surfactant containing) samples. The primary MCM-41 exhibits a spectrum typical of normal MCM-41 and a Q^4/Q^3 ratio of 1.4 compared to a ratio of 3.4 for secondary MCM-41. This indicates that even prior to calcination the pore walls of secondary MCM-41 are made up of fully condensed Q^4 silica units with a small contribution from incompletely cross-linked Q^3 units and hardly any Q^2 units. This is further supported by our observation that on calcination the basal spacing of the primary MCM-41 reduced by 8.0% compared to a reduction of 2.5% for the secondary MCM-41. It is generally accepted that a higher extent of contraction is an indication of a less polymerised or cross-linked framework which therefore undergoes greater dehydroxylation. The TGA and NMR studies are therefore in support of our suggestion that the primary MCM-41 remains largely intact during the secondary synthesis. Furthermore the fact that the final basal spacing of the samples remains largely unaffected suggests that basically the same structural backbone is expanded during the secondary synthesis.

Taken together our results point to a scenario whereby the primary MCM-41 crystallites are largely preserved and act as seeds for further MCM-41 growth during secondary synthesis. For a seeding mechanism to be operative, the primary MCM-41 crystallites must be preserved. To obtain further evidence in support of our proposed seeding mechanism and to show that MCM-41 seed is preserved during secondary synthesis we perfomed some tests and comparisons. The first test was based on the expectation that the seeding mechanism should not work with an MCM-41 material of different d_{100} spacing (or lattice parameter). We prepared large pore MCM-41 by extending the time allowed for crystallisation during primary synthesis from 48 hours to 96 hours.[7–10,18] The resulting material, designated MCM-41(96),[18] had a larger d_{100} spacing of 60.0 Å and a corresponding lattice parameter of 69.3 Å[18] (it is worth noting that as a general rule crystallisation for 48 hours results in MCM-41 with basal spacing of *ca.* 45 Å while 96 hours crystallisation yields ≈60 Å materials).[18] The calcined large pore MCM-41(96) was then used as the silica source for secondary synthesis as described in the experimental section. Since the secondary synthesis step allowed for only 48 hours crystallisation, any 'new' MCM-41 formed would have a d_{100} spacing lower than that of MCM-41(96). Therefore, if the large pore MCM-41(96) were to be completely dissolved during secondary synthesis, then only one MCM-41 phase with the lower d_{100} spacing would be obtained. However, if the MCM-41(96) were to be preserved, then two MCM-41 phases would be observed, *i.e.*, the preserved MCM-41(96) and the new MCM-41 with a lower d_{100} spacing. Furthermore if the MCM-41(96) were to be subjected to secondary recrystallisation for 96 hours, then only one MCM-41 phase with the higher d_{100} spacing would be observed since the preserved and new MCM-41 would have similar d_{100} spacings. This is indeed what is observed as shown in Fig. 8. The XRD pattern of MCM-41(96) recrystallised for 48 hours exhibits two (100) peaks (Fig. 8A); we assign the peak at lower 2θ (59.1 Å) to the preserved large spacing MCM-41(96) and the other peak (46.5 Å) to the new lower spacing MCM-41. Indeed using SEM we were able to observe the two different phases (see electronic supplementary information (ESI)). However when the MCM-41(96) was recrystallised for 96 hours the resulting material had an XRD pattern which exhibits only one slightly broadened (100) peak at 59.2 Å (see Fig. 8B). SEM confirmed the presence of only one MCM-41 phase in this material (see ESI).

The second test was based on the assumption that if total dissolution of the entire 'seed' occurred during secondary synthesis, we would obtain the *same* MCM-41 product regardless of the type of seed used as the silica source, *i.e.*, recrystallisation of primary MCM-41 (designated here as MCM-41(48)) or MCM-41(96) would yield a similar MCM-41 product. This is clearly not the case as shown by a

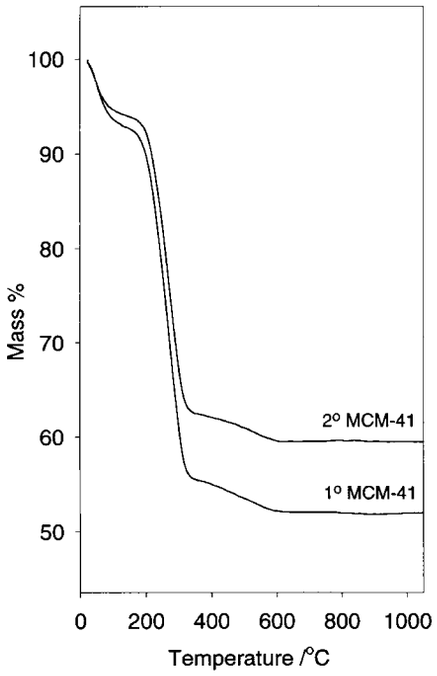

Fig. 6 Thermogravimetric analysis curves for as-synthesised primary (1°) MCM-41 and secondary (2°) MCM-41.

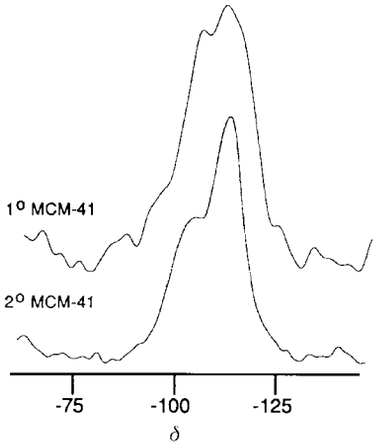

Fig. 7 ^{29}Si MAS NMR spectra of as-synthesised primary (1°) MCM-41 and secondary (2°) MCM-41.

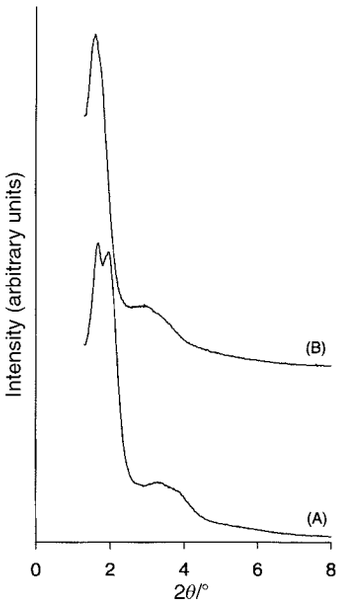

Fig. 8 Powder XRD patterns of calcined (A) MCM-41(96) recrystallised for 48 hours and (B) MCM-41(96) recrystallised for 96 hours.

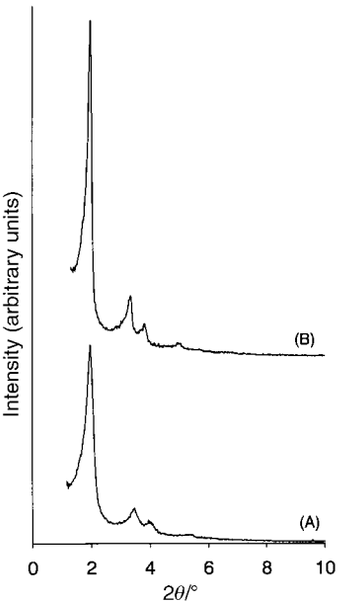

Fig. 9 Powder XRD patterns of calcined (A) primary (1°) MCM-41 and (B) primary (1°) MCM-41 recrystallised for 96 hours.

comparison between Fig. 1B and Fig. 8A. Recrystallisation of MCM-41(48) for 48 hours yields secondary MCM-41 (Fig. 1B) which is entirely different from the two phase MCM-41 material (Fig. 8A) obtained from a similar recrystallisation of MCM-41(96). This implies that the seed crystallites determine the product of recrystallisation. Furthermore we investigated the effect of 96 hours recrystallisation on MCM-41(48) and MCM-41(96) seed. It is worth pointing out here that if, as we suggest, a mechanism other than trivial dissolution of the entire seed was operative, then the product of 96 hour recrystallisation of MCM-41(48) seed would differ from that of MCM-41(96) recrystallised over the same time. We have already shown that MCM-41(96) seed recrystallised over 96 hours yields a large spacing MCM-41 material (see Fig. 8B). This contrasts with Fig. 9 which shows the XRD pattern of MCM-41(48) before and after recrystallisation for 96 hours. It is clear from Fig. 9 that; (i) only one MCM-41 phase is obtained, (ii) no large spacing MCM-41 material is obtained despite 96 hours recrystallisation and (iii) the d_{100} spacing of the seed MCM-41 is retained in the recrystallised sample. It is particularly interesting that recrystallisation of MCM-41(48) seed for 96 hours does not, despite the longer secondary synthesis time, result in large spacing MCM-41.[7–10,18] The presence of the MCM-41(48) seed clearly prevents the formation of the large pore MCM-41 typical of 96 hour synthesis.[7–10,18] This is only possible if the main operative mechanism during the recrystallisation involves preservation of seed crystallites which then provide the backbone for any further MCM-41 formation.

A pore channel formation and/or crystal growth mechanism[19] may be invoked to explain the observed crystal growth, pore wall thickening and morphological transformation. During recrystallisation silicate units may enter the pores of the 'seed' primary MCM-41 crystallites thereby increasing both the thickness of the pore walls and the proportion of Q^4 silica units *via* further condensation in a process similar to silylation. Silicate units also interact with the additional surfactant molecules on the outer surface of the 'seed' crystals forming new surfactant/silica aggregates which extend growth in the *ab* plane. The new surfactant/silica aggregates may then act as linkages between seed primary MCM-41 crystallites thereby forming larger crystallites. The formation of a sheet-like morphology suggests that the 'seed' particles are predominantly connected *along* (side-on) each other rather than *on* each other. In such a scenario only a small amount of 'new silica' as silicate ions is required to act as bridges in the formation of larger particles. Furthermore, whilst it is unlikely that the surfactant molecules will enter the pores of the 'seed' crystals they may however interact with silicate units at the pore mouth to extend growth in the *c*-direction. The proposed crystal enlargement process is schematically illustrated in Fig. 10. The all-round crystal growth (with the crystallites of the primary MCM-41 acting as 'seeds') results in better long range ordering and thicker pore walls but with no significant change in lattice parameter (a_o) since the wall thickness increases within the confines of the existing primary MCM-41 pores. It is conceivable that extensive crystal growth would result in the apparent transformation from sphere shaped to sheet or plate like particles.

Conclusions

This report demonstrates that it is possible to prepare large crystallite purely siliceous MCM-41 materials with improved long range structural ordering *via* a simple two step synthesis procedure. The procedure which utilises calcined (primary) MCM-41 as the 'silica source' facilitates both structural and morphological changes. There is strong evidence that the calcined MCM-41 used as the silica source is preserved during secondary synthesis and that its crystallites act as seeds for further crystal growth. Although we do not rule out dissolution

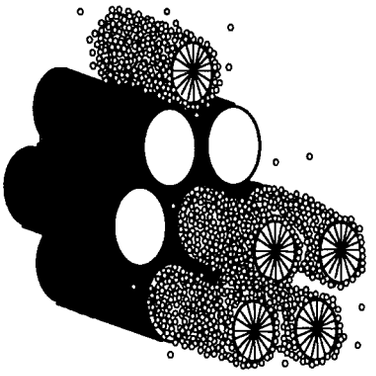

Fig. 10 Schematic illustration of the enlargement of a calcined primary MCM-41 crystallite seed during secondary synthesis.

of part of the primary MCM-41, it seems likely that further growth is facilitated by the dissolution of the amorphous silica phase which is part of the primary MCM-41 yield; the amorphous silica phase is therefore the real source of silicate ions which are neccesary for crystal enlargement. In addition to having larger crystallites, the resulting 'secondary' MCM-41 exhibits much better long range structural ordering as observed by powder XRD and TEM. The secondary synthesis also causes a modest increase in basal (d_{100}) spacing and a decrease in pore size resulting in thicker pore walls and a slight decrease in surface area and pore volume. It is thought that pore wall thickening occurs when silicate units diffuse into the pores of the seed primary MCM-41 crystallites thereby increasing both the thickness of the pore walls and the proportion of Q^4 silica units *via* further condensation in a process similar to silylation. Only limited changes in the basal spacing and lattice parameter occur since the wall thickness increases within the confines of the existing primary MCM-41 pores. These structural changes are accompanied by an apparent change in morphology from sphere shaped particles to larger sheet or plate like domains. The TGA, ^{29}Si NMR, SEM and powder XRD studies presented provide very strong evidence for a seeding mechanism.

Acknowledgements

R.M. is grateful to the EPSRC for an Advanced Fellowship and the Royal Society for an equipment grant. The assistance of Y. Khimyak with the NMR measurements is appreciated.

References

1 J. Y. Ying, C. P. Mehnert and M. S. Wong, *Angew. Chem,. Int. Ed.*, 1999, **38**, 56.
2 J. S. Beck, J. C. Vartuli, W. J. Roth, M. E. Leonowizc, C. T. Kresge, K. D. Schmitt, C. T-W. Chu, D. H. Olson, E. W. Shepard, S. B. McCullen, J. B. Higgins and J. L. Schlenker, *J. Am. Chem. Soc.*, 1992, **114**, 10834.
3 M. Kruk, M. Jaroniec and A. Sayari, *J. Phys. Chem. B*, 1997, **101**, 583.
4 P. T. Tanev and T. J. Pinnavaia, *Chem. Mater.*, 1996, **8**, 2068.
5 Q. Hou, D. I. Margolese and G. D. Stucky, *Chem. Mater.*, 1996, **8**, 1147.
6 A. Galarneau, D. Desplantier, R. Dutartre and F. Di Renzo, *Microporous Mesoporous Mater.*, 1999, **27**, 297.
7 D. Khushalani, A. Kuperman, G. A. Ozin, K. Tanaka, J. Garces, M. M. Olken and N. Coombs, *Adv. Mater.*, 1995, **7**, 842.
8 C.-F. Cheng, W. Zhou and J. Klinowski, *Chem. Phys. Lett.*, 1996, **263**, 247.
9 A. Corma, Q. Kan, M. T. Navarro, J. Perez-Pariente and F. Rey, *Chem. Mater.*, 1997, **9**, 2123.
10 A. Sayari, P. Liu, M. Kruk and M. Jaroniec, *Chem. Mater.*, 1997, **9**, 2499.
11 L. Chen, T. Horiuchi, T. Mori and K. Maeda, *J. Phys. Chem. B*, 1999, **103**, 1216.
12 M. Kruk, M. Jaroniec and A. Sayari, *Microporous Mesoporous Mater.*, 1999, **27**, 217.
13 R. Ryoo and J. M. Kim, *J. Chem. Soc., Chem. Commun.*, 1995, 711.
14 K. J. Elder and J. W. White, *Chem. Mater.*, 1997, **9**, 1226.
15 R. Mokaya, W. Zhou and W. Jones, *Chem. Commun.*, 1999, 51.
16 J. M. Kim, S. K. Kim and R. Ryoo, *Chem. Commun.*, 1998, 259.
17 C.-F. Cheng, D. H. Park and J. Klinowski, *J. Chem. Soc., Faraday Trans.*, 1997, **93**, 193.
18 R. Mokaya, *J. Phys. Chem. B*, 1999, **103**, 10204.
19 W. Zhou and J. Klinowski, *Chem. Phys. Lett.*, 1998, **292**, 207.